

## **MODELING OF RESIDUAL STRESS EFFECTS USING EIGENSTRAIN**

Michael R. Hill

Mechanical and Aeronautical Engineering, University of California,  
One Shields Avenue, Davis, CA 95616, USA, mrhill@ucdavis.edu

### **ABSTRACT**

This paper discusses the modeling of residual stresses in fracture problems. Historically, residual stress effects in fracture have focused on the crack driving force, so that solely opening mode residual stresses are assumed to influence fracture. However, residual stresses can effect all components of stress at the crack-tip, and can thereby alter crack-tip constraint and influence material toughness. This paper discusses a modeling approach capable of revealing the effects of residual stress on both driving force and constraint. The modeling employs non-linear finite element analyses in which residual stresses are treated using eigenstrain. Eigenstrain is imposed to induce residual stress as an initial condition in a cracked geometry. Under subsequent applied loading, the stress fields due to applied and residual loadings are free to interact, with residual stress being potentially reduced by gross plasticity. In order to predict fracture independent from the level of crack driving force, the evolution of the crack-tip stress and strain with applied loading is monitored using any of various micromechanical fracture prediction schemes, which depend directly on the crack-tip conditions. Domain integral solutions for  $J$ , derived from the FEM results and properly corrected for the presence of initial eigenstrain, are computed. Constraint is quantified using  $J$ - $Q$  theory. Together,  $J$  and  $Q$  allow comparison between the modeling approach pursued and more traditional global parameter approaches.

### **KEYWORDS**

residual stress, fracture, eigenstrain, finite element method

### **INTRODUCTION**

Recent research in micromechanical modeling has made progress toward the accurate prediction of fracture under various crack-tip constraint conditions. Historically, fracture prediction has focused on determining a global fracture parameter (e.g., the  $J$ -integral,  $J$ , or the Mode-I stress intensity factor,  $K_I$ ) as a function of applied load, and finding the load at which the parameter exceeds a critical level for fracture. This approach rests on the assumption that the fracture parameter alone controls the crack-tip stress and strain. Unfortunately, in application, material non-linearity (i.e., yielding) at the crack-tip invalidates this assumption. Yielding is a function of the triaxial state of stress, and the crack-tip stress state has a range of variation in real structures. In fact, it is well known that differences in crack-tip triaxiality (or, more commonly “constraint”) can exist in structures due to differences in geometry and applied loading (e.g., thick versus thin, or tension versus bending). Further, different crack-tip stresses lead to fracture at different levels

of the global fracture parameter. An alternative method to parameter-based approaches, micromechanical methods directly examine the crack-tip stress and strain state to provide an estimate of fracture propensity. Implementation of the micromechanical approach therefore requires the prediction of crack-tip stress and strain, and its history with applied loading. In practice, finite element methods (FEM) are used to compute the crack-tip conditions, as a function of applied loading.

Application of the micromechanical approach to predict fracture in residual stress bearing structures provides some surprising results. The traditional approach to predict fracture of residual stress (RS) bearing, flawed components involves linear superposition. This approach assumes that only opening mode RS will impact the fracture process, when, in fact, residual stresses are often triaxial. Triaxial RS will influence non-linear material behavior at the crack-tip, a process not accounted for by superposition. Including RS in a micromechanical approach, however, does allow the residual stress field to affect the behavior of material at the crack-tip. Accordingly, the micromechanical approach offers a more complete accounting of RS effects in fracture, and gives insight to the fracture process when RS is present. An example application of this approach is briefly described, which illustrates the alteration of driving force and constraint due to residual stress, and their effect on fracture prediction.

## FRAMEWORK

This section describes a computational and analytical framework for predicting fracture in flawed, RS bearing structures using micromechanics. We first lay out the general finite element procedures employed. Next, we describe methods for introducing RS into the computation. The computational results provide the crack-tip stress and strain history as a function of applied load, which serve as input to a micromechanical fracture prediction model. The RKR model for brittle fracture is described, and later used to illustrate the approach. Finally,  $J$ - $Q$  analysis is described, which helps to interpret the stress and strain history at the crack-tip, and to compare the results of micromechanics to those that would be obtained using a traditional global parameter approach.

### *General analysis techniques*

Elastic-plastic finite element computation is used to simulate the response of a structure of interest to both applied and residual stresses simultaneously. The finite element solutions employ a non-linear, finite strain formulation. Plasticity is assumed to follow isotropic, incremental  $J_2$  flow theory with a piece-wise linear Cauchy-stress logarithmic-strain curve obtained from tensile testing. Commercial codes can be used to perform these analyses. Mesh refinement in the crack-tip region is critical, and must assure that stress and strain are accurately captured in the near crack-tip region. Time-stepping in the analysis provides a means to capture the developing crack-tip state with increasing applied load, which serves as input to the fracture prediction scheme.

### *Inclusion of residual stress*

Residual stress is included in the finite element computation using eigenstrain,  $\epsilon^*$ . Eigenstrain is a combination of all the non-elastic, incompatible strains set up during processing of a material [1]. In welding, the eigenstrain is a combination of thermal, plastic, and transformation strains; in coining or autofrettage, the eigenstrain is due to plasticity. The eigenstrain field is defined with reference to *elastic* deformation of the structure, and reproduces the entire RS state when the material behavior is *elastic*; therefore, eigenstrain is *not* merely a sum of the various non-linear strains. For a particular process, the eigenstrain field is a tensor with spatial dependence, and can be found experimentally [2] or by modeling [3]. If a process model is used to determine the residual stress field in a given body,  $\sigma^{RS}$ , or if residual stress is measured at enough points to provide a spatial distribution of the residual stress field, the eigenstrain field can be found from the residual stress field using

$$\epsilon_{ij}^* = -C_{ijkl}^{-1} \sigma_{kl}^{RS} \quad (1)$$

where  $C$  is the usual elastic tensor giving stress from elastic strain.

The use of an eigenstrain distribution in modeling offers several advantages for further analysis. First, the residual stress present can be determined by imposing the eigenstrain distribution in a linear elastic finite element model of the geometry. (Note that residual stresses, by their nature, do not result in active yielding, and a valid eigenstrain field must impose stresses that satisfy the yield criterion). Although an eigenstrain analysis is complicated by the spatial variation of each component of the eigenstrain tensor, a general-purpose finite element program can be used to produce the RS field. Further, when the eigenstrain field is known, the entire, full-field, triaxial RS state is known at every point within the structure.

When the eigenstrain field is known for the unflawed structure, the analysis of a flawed structure can be performed. The addition of a crack introduces new surfaces, and the RS state in the flawed body depends on these surfaces. If the structure is linear elastic, the state is found simply by modeling the traction-free surfaces. In non-linear materials, crack-tip yielding must be allowed when introducing the flaw. To handle this situation, the eigenstrain distribution is first imposed in the body with crack-face nodes restrained, and the equilibrium RS state found (this step is elastic). Then, the crack-face nodes are released in succession, so that the crack gradually extends from the free surface to simulate fatigue (this step can be elastic-plastic). The rate at which the crack is extended will have a bearing on the crack-tip fields, and one must ensure that the opening is gradual enough (e.g., so subsequent fracture analysis is not affected). When properly executed, this process redistributes the original RS field, allowing for crack-tip yielding, and resulting in a flawed RS bearing structure.

Once RS is introduced into the computation, applied loading is simulated. During this subsequent loading phase, the residual and applied stresses act together at the material level. Any new plastic deformation is the result of both stress types. Therefore, this analysis technique allows for the non-linear interaction of RS and applied loading, which is not accounted for when applying global approaches.

An alternative to using eigenstrain is direct simulation the process causing the residual stress field. Results of the simulation can then be used as an initial condition for the simulation of crack introduction and applied loading. However, direct simulation can only be readily pursued for simple problems, with small amounts of plasticity or other incompatible strain.

### ***Micromechanical fracture prediction***

Since the analysis technique just described provides a complete description of the material state in the presence of residual and applied loading, the crack-tip material history can be used within a micromechanical scheme to predict fracture. The physical phenomena occurring in the fracture process vary, and it is generally useful to consider brittle and ductile fracture processes separately [4]. Here we briefly describe one model for predicting brittle fracture, and this is used later to illustrate the general computational approach. In principle, other micromechanical models could be employed.

Initiation of cleavage fracture in mild steels can be predicted using the RKR micromechanical model [5]. This simple model predicts fracture when the opening stress,  $\sigma_{yy}$ , ahead of the crack-tip exceeds a fracture stress,  $\sigma_f^*$ , over a microstructurally relevant distance,  $l^*$ . In applying this model, one monitors the progress of the opening stress ahead of the crack-tip due to residual and applied loading. Once the RKR criterion is satisfied, fracture is predicted. The parameters in the RKR model are typically found through laboratory testing for a given material and reported ranges for steels are 2 to 5 grain diameters for  $l^*$ , and 2 to 4 times the yield strength for  $\sigma_f^*$  [5]. When the micromechanics condition for fracture initiation is satisfied, the associated applied load and global fracture parameters (e.g.,  $J$ -integral) can be found from the FEM results.

### ***Characterization of crack-tip behavior***

When the above procedures are used to predict fracture, none of the traditional global fracture parameters are used. Nevertheless, it is useful to compare the micromechanical predictions with those that might be made using a traditional approach. To perform this comparison, we utilize two parameters, one related to driving force and one to constraint. Specifically, we invoke  $J$ - $Q$  theory, which was developed from simulation of crack-tip fields in finite and infinite size bodies [6,7].

During the non-linear analysis, the  $J$ -integral is estimated at each increment of applied loading using the domain integral technique. As such, the computed value of  $J$  includes the contribution of residual stress within the material. Calculation of  $J$  in the presence of RS and eigenstrain requires special attention. Recent work [8,9,10] has found that domain-independent values of  $J$  can be obtained if two corrections are made to the usual domain integral formulation for  $J$ . The first of these involves the spatial derivative of the residual stress or eigenstrain field with respect to the crack driving direction (assumed to be  $x_1$  here, for simplicity) [8]. The second involves a modification of the work density of the material,  $W$ , to account for plastic dissipation present at a crack-free initial state, which follows residual stress introduction,  $W_{\text{initial state}}^p$  [9]. The first correction term is required to obtain domain independence in any modeling approach that involves residual stress or eigenstrain. The second term is needed, for example, when the residual stress state is found through process modeling which causes plastic straining and dissipation unrelated to subsequent fracture loading. The domain integral including these two additional terms can be written as [10]

$$J = \frac{1}{A_q} \left( \int_V \left( \sigma_{ij} \frac{\partial u_j}{\partial x_1} \frac{\partial q}{\partial x_i} - W \frac{\partial q}{\partial x_1} \right) dV + \int_V \left( \sigma_{ij} \frac{\partial (\epsilon_{ij}^* - C_{ijkl}^{-1} \sigma_{kl}^{RS})}{\partial x_1} \right) q dV + \int_V \left( W_{\text{initial state}}^p \frac{\partial q}{\partial x_1} \right) dV \right) \quad (2)$$

where the first integral is the usual domain integral formulation for  $J$ , and the second and third integrals are the first and second correction terms described above; these three terms, including the leading factor  $1/A_q$ , will be referred to as  $J_1$ ,  $J_2$ , and  $J_3$ . The quantities in the integrals not yet defined are the stress tensor,  $\sigma_{ij}$ , the displacement vector,  $u_j$ , the spatial coordinates,  $x_i$ , a scalar weight function representing a virtual displacement,  $q$ , the material work density,  $W$ , and the crack-front area of the virtual displacement,  $A_q$  (see, e.g., [11]).

In a number of cases, the values of  $J$  computed from the usual formulation (i.e.,  $J_1$  alone) are highly inaccurate. Consider, for example, the cold-expanded hole with a radial crack shown in Figure 1(a) which was recently studied in [12]. In that study, the uncracked hole was expanded radially by 4%, then allowed to relax to form a compressive residual stress field at the hole periphery. The radial cracks shown in the figure were then introduced, and far-field loading applied. Because the residual stress varied strongly near the hole, and because the plasticity caused by the expansion process introduces plastic dissipation unrelated to the fracture problem, the  $J$  values published in [12] were highly domain-dependent. Reproducing the simulations, and computing the three terms in Eqn. 2, provides the results shown in Figure 1(b) [10]. Clearly the correction terms in Eqn. 2 are important for obtaining domain independence of  $J$  in such problems.

For a given level of  $J$ , the constraint conditions at the crack-tip are represented by the parameter  $Q$ .  $Q$  has been shown to characterize the magnitude of the hydrostatic stress over the forward sector ahead of the crack-tip to a good approximation.  $Q$  is formally defined as

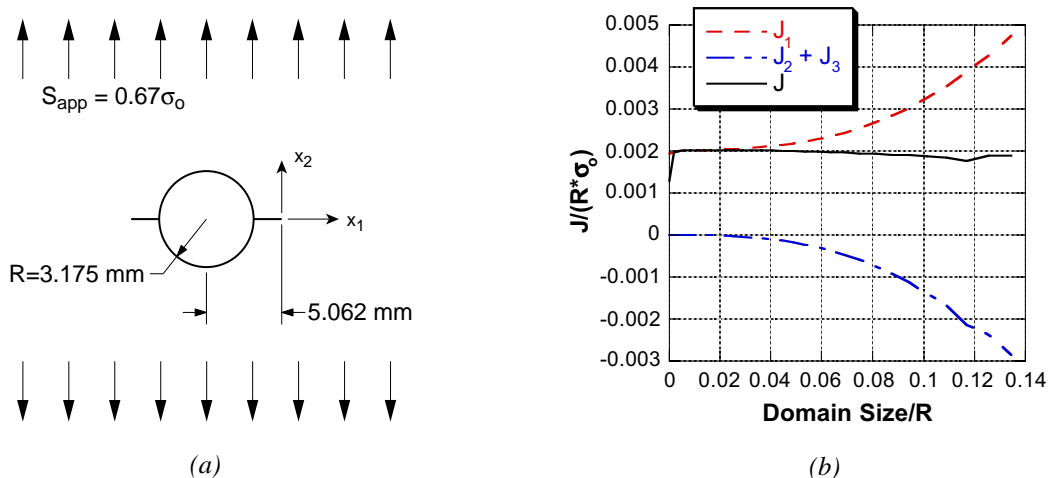


**Figure 1:** Cold expanded hole with radial crack: (a) geometry, and (b) domain integral results

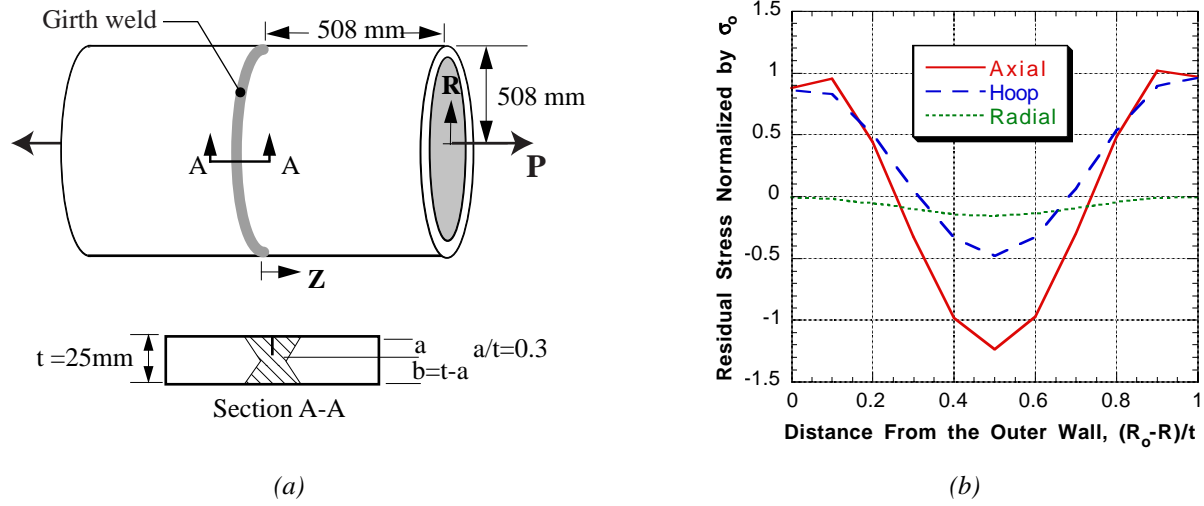


**Figure 2:** (a) Girth-welded pressure shell, (b) RS in the unflawed condition

$$Q = \left( \frac{\sigma_{\theta\theta} - \sigma_{\theta\theta}|_{SSY; T=0}}{\sigma_o} \right) \text{ at } \theta = 0, \left( \frac{r\sigma_o}{J} \right) = n \quad (3)$$

where,  $\sigma_o$  is the material yield strength, and  $n$  is a constant usually taken in the range 2 to 4 [6,7].  $Q$  depends on the crack-tip stress state in the body of interest,  $\sigma_{\theta\theta}$ , and on the stress state in a plane-strain, Mode I loaded, small-scale yielding reference solution,  $\sigma_{\theta\theta}|_{SSY; T=0}$ , where both exhibit the same  $J$ .

Because  $Q$  is a constraint parameter, it provides insight into the fracture process.  $Q$  near zero suggests that a body is in small-scale yielding. As deformation levels increase in finite specimens, the hydrostatic stresses at the crack-tip are relieved, producing a negative  $Q$  value, and signaling a loss in constraint. A negative value of  $Q$  indicates lower crack-tip stress compared to a body in small-scale yielding and, therefore, a reduced propensity for cleavage fracture at a given value of  $J$ . A positive  $Q$ -value indicates that high constraint exists for a particular crack-tip state.

## TRIAxIAL STRESS EFFECTS IN BRITTLE FRACTURE

This section serves as an example to illustrate the approach described above. It focuses on the prediction of brittle fracture of the axially loaded, girth-welded shell shown in Figure 2(a), initiating from a circumferential external flaw. Details of the study can be found in [13]. The properties assumed are those of A516-70, a high hardening, ferritic, pressure vessel steel with uniaxial yield strength of 303 MPa. The RKR parameters for this material are assumed to be  $\sigma_f^* = 3.5\sigma_o$  and  $l^* = 0.15$  mm, or about 3 ferritic grain diameters.

This analysis makes use of an assumed eigenstrain distribution. This distribution gives rise to residual stresses that are typical of a continuously welded, double-sided joint in mild steel plate [14]. The nature of continuous welding allows the assumption of an eigenstrain field that depends on the transverse and through-thickness welding directions, but is independent of position along the weld. Further, the eigenstrain field is assumed symmetric about both the centerline of the weld and the mid-wall of the shell. The residual stress field computed when the assumed eigenstrain field is imposed in the un-flawed geometry is shown in Figure 2(b), on the plane where the crack will be introduced. For the flaw orientation shown in Figure 2(a), axial stresses correspond to the opening mode, and over the length of defect considered (from 0 to 0.3 in Figure 2(b)), the axial RS is tensile. Accordingly, RS will tend to increase the crack-driving force and therefore decrease the fracture load.

Fracture predictions using the RKR model show a strong constraint effect caused by RS. Fracture loads are predicted to be 21.3 MN and 9.83 MN without and with RS, respectively. Because RKR is satisfied at these loads, crack-tip opening stresses are nearly the same in each loading case. However, this occurs at markedly

different values of  $J$ , 36.7 kN/m without RS and 13.5 kN/m with RS. Recall that these values of  $J$  are computed using the domain integral, so they include the influence of RS on driving force. As shown in Figure 3(a), the significant change in  $J$  at fracture is due to high constraint imposed by the RS field. Figure 3(b) shows that this additional constraint suppresses plastic strain formation compared with the non-residual stress bearing case. These interesting results demonstrate that RS can cause a significant change in crack-tip constraint. Figure 3(a) shows that the tension loaded shell has quite low constraint when RS is absent, but behaves like a body in small-scale yield when RS is present. If the RS bearing shell were assumed to have constraint similar to the RS-free shell, the superposition approach would lead to an erroneous and non-conservative fracture assessment. This observation gives credence to codified assumptions of high constraint, as RS can combine with applied loads to produce highly constrained crack-tip fields in a geometry and loading condition that would otherwise exhibit low constraint.

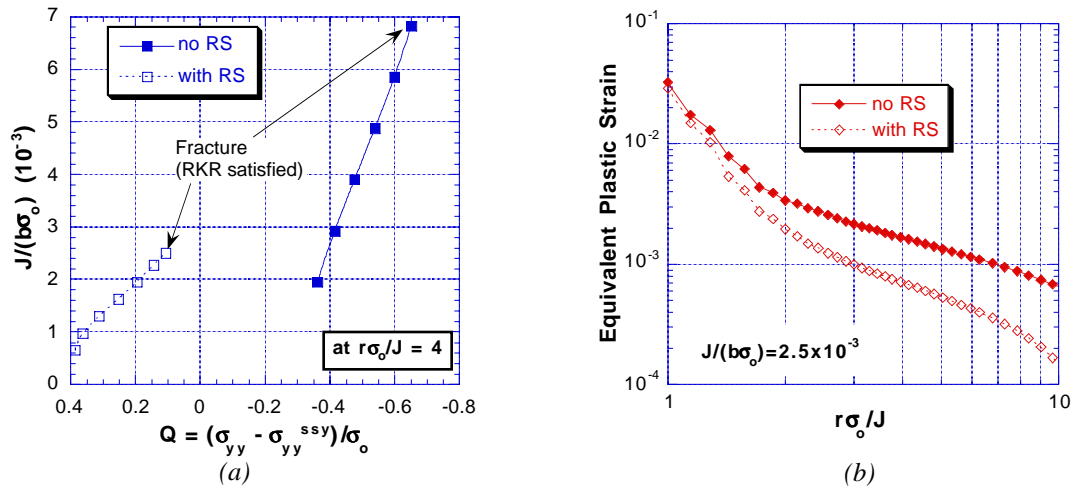


Figure 3: (a)  $J$ - $Q$  trajectories and (b) plastic strain for the shell

## REFERENCES

1. Mura, T. (1987). *Micromechanics of Defects in Solids*. Dordrecht, Netherlands.
2. Hill, M.R. (1996). Ph.D. Thesis, Stanford University.
3. Goldak, J.A., and Patel, B. (1985). In: *Advanced Joining of Materials (AGARD CP-398)*, pp. 1-1 - 1-32. AGARD.
4. Shih, C.F. (1999). In: *Fatigue and Fracture Mechanics, 29th Volume*, pp. 9-14, Panontin, T.L., and Sheppard, S.D., Eds. ASTM, West Conshohocken, PA.
5. Ritchie, R.O., Server, W.L., and Wullarert, R.A. (1979) *Met Trans A* 10, 1557.
6. O'Dowd, N.P., and Shih, C.F. (1991) *J Mech Phys Solids* 39, 989.
7. O'Dowd, N.P., and Shih, C.F. (1992) *J Mech Phys Solids* 40, 939.
8. Matos, C.G., and R. H. Dodds, Jr. (2000) *Eng Struct* 22, 1103.
9. Lei, Y., O'Dowd, N.P., and Webster, G.A. (2000) *Int J Fract* 106, 195.
10. Meith, W.A. (2001). MSc Thesis, University of California, Davis.
11. Shih, C.F., Moran, B., and Nakamura, T. (1986) *Int J Fract* 30, 79.
12. Pavier, M.J., Poussard, C.G.C., and Smith, D.J. (1999) *Eng Fract Mech* 63, 751.
13. Panontin, T.L., and Hill, M.R. (1996) *Int J Fract* 82, 317.
14. Gunnert, R. (1961). In: *Proceedings of the Special Symposium on the Behavior of Welded Structures*, pp. 164-201, Kingery, R.A., Ed. University of Illinois Engineering Experiment Station, Urbana, IL.